Selective CO_2-to-formate electrochemical conversion with core-shell structured Cu_2O/Cu@C composites immobilized on nitrogen-doped graphene sheets

Da Li,[ab] Tongtong Liu,[b] Linlin Huang,[b] Jing Wu,[b] Jiannan Li,[b] Liang Zhen,*[a,c,d] and Yujie Feng[b]*

[a] School of Materials Science and Engineering, Harbin Institute of Technology (Shenzhen), Shen Zhen 518055, China

[b] State Key Laboratory of Urban Water Resource and Environment, Harbin Institute of Technology, Harbin 150090, China

[c] MOE Key Laboratory of Micro-Systems and Micro-Structure Manufacturing, Harbin Institute of Technology, Harbin 150080, China

[d] School of Material Science and Engineering, Harbin Institute of Technology, Harbin 150001, China

*Corresponding Author: lzhen@hit.edu.cn (*L. Zhen*),
yujief@hit.edu.cn (*Y. -J. Feng*)

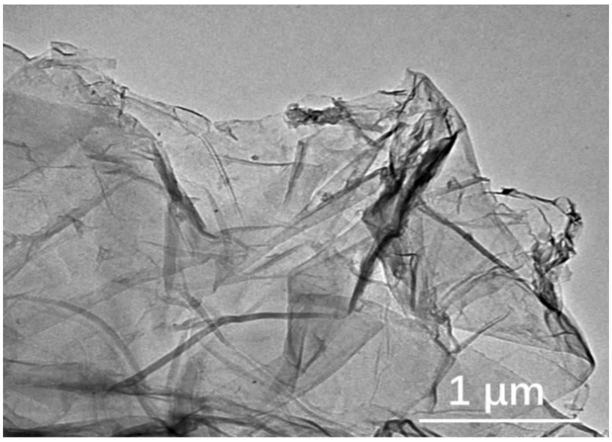

Figure S1 TEM N-doped reduced graphene oxide.

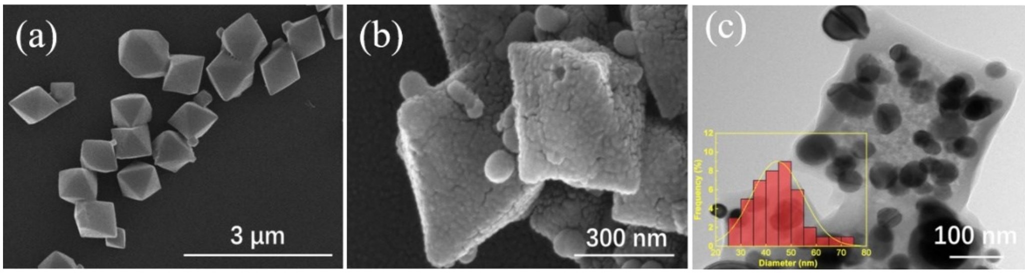

Figure S2 SEM image of Cu_btc particles (a), SEM (b) and TEM images (c) after Cu_btc carbonization, insertion presented the size distribution of metallic nanoparticle.

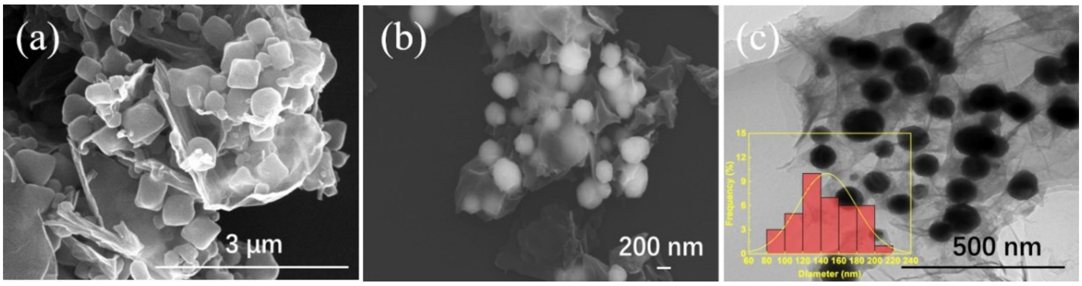

Figure S3 SEM image of Cu_btc/rGO composites (a), SEM (b) and TEM images (c) after Cu_btc/rGO carbonization, insertion presented the size distribution of metallic nanoparticle.

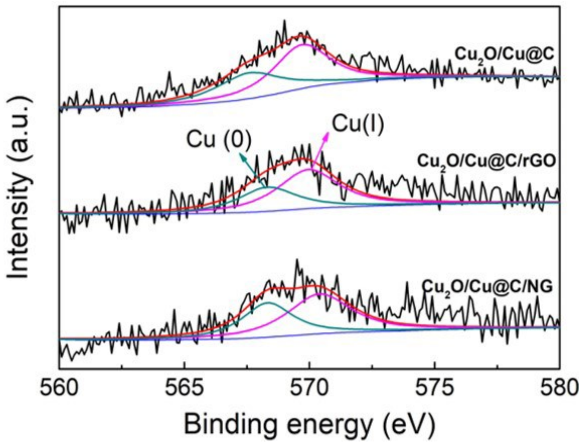

Figure S4 Cu LMM Auger spectra of Cu_2O/Cu@C, Cu_2O/Cu@C/rGO, and Cu_2O/Cu@C/NG.

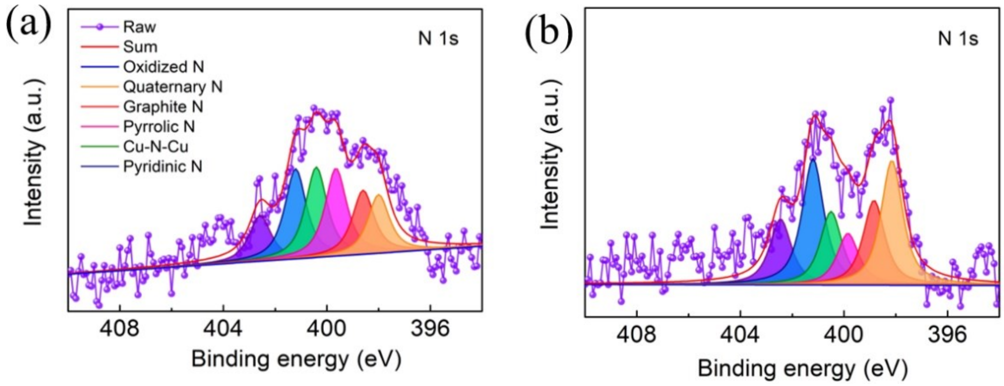

Figure S5 Higher resolution of XPS N 1s of Cu_2O/Cu@C (a) and Cu_2O/Cu@C/rGO (b).

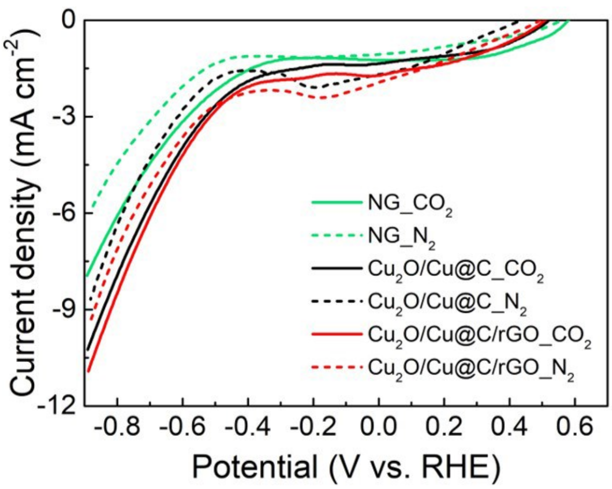

Figure S6 LSV curves for NG, Cu_2O/Cu@C, and Cu_2O/Cu@C/rGO in N_2- and CO_2-saturated 0.1 M $KHCO_3$ electrolyte.

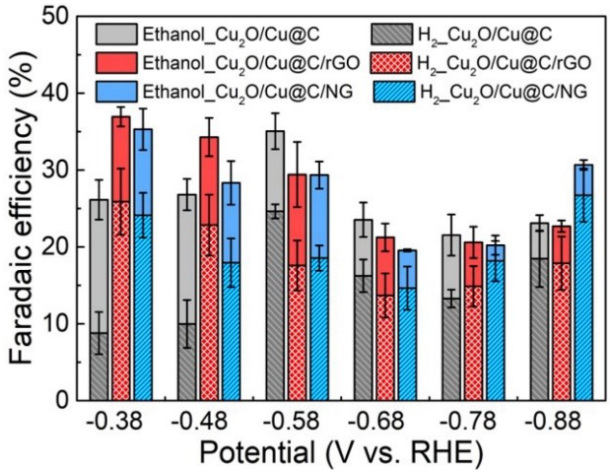

Figure S7 Faradaic efficiency for hydrogen and ethanol of Cu_2O/Cu@C, Cu_2O/Cu@C/rGO, and Cu_2O/Cu@C/NG.

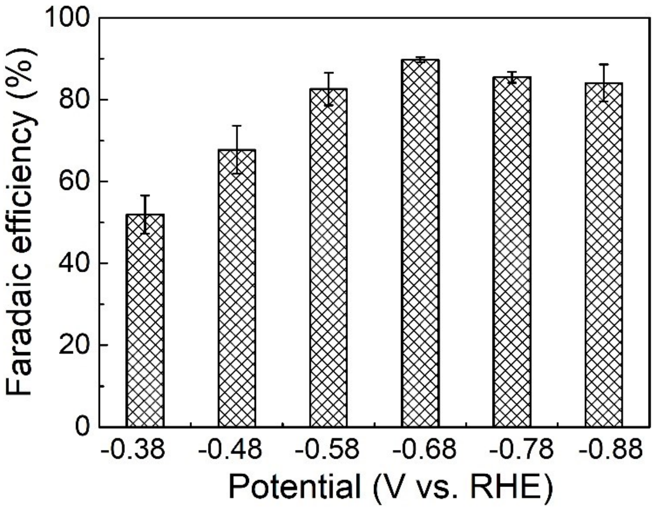

Figure S8 Faradaic efficiency for hydrogen of NG.

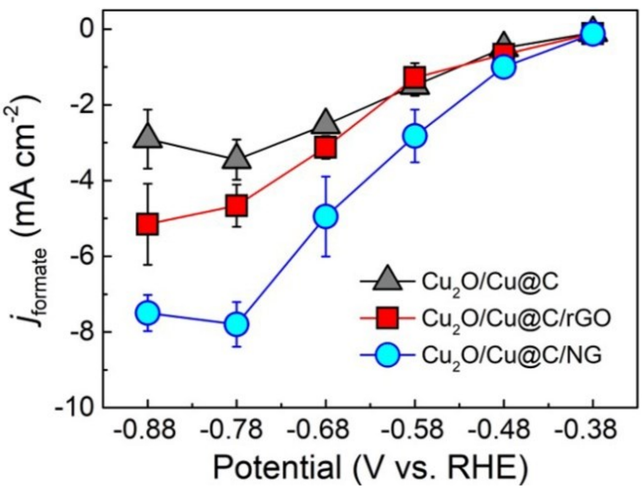

Figure S9 Partial current density of formate for Cu_2O/Cu@C, Cu_2O/Cu@C/rGO, and Cu_2O/Cu@C/NG.

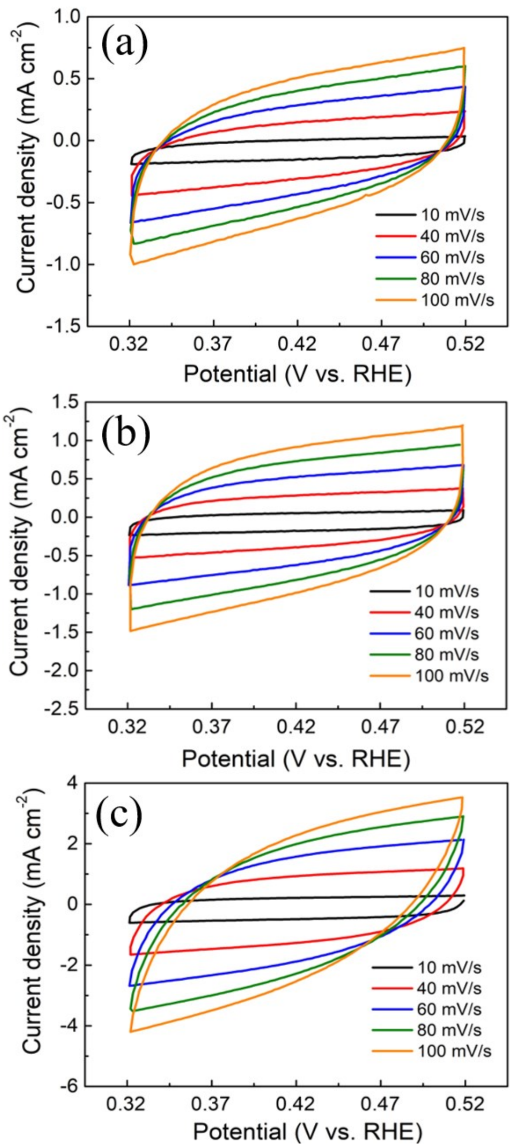

Figure S10 Cyclic voltammagrams at scan rate range from 10 to 100 mV s^{-1} for Cu_2O/Cu@C (a), Cu_2O/Cu@C/rGO (b), and Cu_2O/Cu@C/NG (c), respectively.

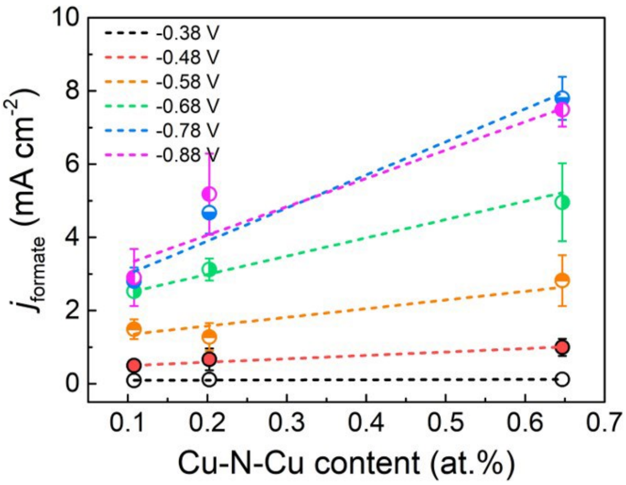

Figure S11 The linear fitting between Cu-N-Cu content and partial current density of formate obtained by Cu_2O/Cu@C, Cu_2O/Cu@C/rGO and Cu_2O/Cu@C/NG.

Table S1 Atomic concentration (%) of Cu_2O/Cu@C, Cu_2O/Cu@C/rGO, and Cu_2O/Cu@C/NG

Catalysts	Cu	C	N	O
Cu_2O/Cu@C	0.87	90.37	0.74	8.02
Cu_2O/Cu@C/rGO	0.37	93.26	1.26	5.11
Cu_2O/Cu@C/NG	0.31	88.14	3.97	7.58

Table S2 Atomic concentration (%) of N species in Cu_2O/Cu@C, Cu_2O/Cu@C/rGO, and Cu_2O/Cu@C/NG

Catalysts	pyridinic	pyrrolic	Cu-N-Cu	graphite	quaternar y	oxidized
Cu_2O/Cu@C	0.13	0.13	0.11	0.15	0.14	0.076
Cu_2O/Cu@C/rGO	0.30	0.12	0.20	0.18	0.30	0.16
Cu_2O/Cu@C/NG	0.67	0.46	0.65	0.57	1.12	0.50

Table S3 Internal resistance of Cu_2O/Cu@C, Cu_2O/Cu@C/rGO, and Cu_2O/Cu@C/NG

Catalysts	R_{ohm}	R_{ct}
Cu_2O/Cu@C	4.25	9.91
Cu_2O/Cu@C/rGO	4.77	7.64
Cu_2O/Cu@C/NG	4.79	3.91

Table S4 Performance comparison of CO_2 reduction with reported Cu-based MOF materials or metals loaded on graphene-based substrate

Catalyst	Electrolyte	Potential for FE_{max}	Product and maximum *FE*	Ref.
HKUST-1 derived Cu/C	0.1M $KHCO_3$	–0.3 V vs. RHE	HCOOH: ~10%	1
Cu-NU1000	0.1 M $NaClO_4$	–0.82V vs. RHE	Formate: 28%	2
Cu rubeanate MOF	0.5 M $KHCO_3$	–1.2 V vs. SHE	HCOOH: 30%	3
Cu_2O/Cu@NC-800	0.1 M $KHCO_3$	–0.68 V vs. RHE	Formate: 70.5 %	4
Cu_2O/Cu@C/NG	0.1 M $KHCO_3$	–0.78 V vs. RHE	Formate: 82.8%	This study
GN/ZnO/Cu_2O	0.5 M $NaHCO_3$	–0.9 V vs. Ag/AgCl	n-propanol: 30%	5
SnO_2/rGO	0.5 M $NaHCO_3$	–0.8 V vs. Ag/AgCl	Formate: 89%	6
Bi_2O_3-NGQDs	0.5 M $KHCO_3$	–0.9 V vs. RHE	Formate: ~100%	7
Co/SL-NG	0.1 M $NaHCO_3$	–0.90 V vs. SCE	Methanol: 71.4%	8
Zn–N–G-800	0.5 M $KHCO_3$	–0.5 V vs. RHE	CO: 91%	9
Cu_2O/NRGO	0.1 M $KHCO_3$	–1.4 V vs. RHE	C_2H_4: 19.7%	10

Table S5 Linear fitting between atomic content of Cu-N-Cu (%) in Cu_2O/Cu@C, Cu_2O/Cu@C/rGO, and Cu_2O/Cu@C/NG and the partial current densities

Potential (V)	Linear equation	R^2
-0.38	y=0.051x+0.089	0.83
-0.48	y=0.93x+0.41	0.96
-0.58	y=2.36x+1.10	0.51
-0.68	y=4.99x+1.20	0.95
-0.78	y=9.03x+2.09	0.91
-0.88	y=7.74x+2.52	0.90

1 K. Zhao, Y. Liu, X. Quan, S. Chen and H. Yu, *ACS Appl. Mater. Interfaces*, 2017, **9**, 5302-5311.
2 C. W. Kung, C. O. Audu, A. W. Peters, H. Noh, O. K. Farha and J. T. Hupp, *ACS Energy Letters*, 2017, **2**, 2394-2401.
3 R. Hinogami, S. Yotsuhashi, M. Deguchi, Y. Zenitani, H. Hashiba and Y. Yamada, *ECS Electrochem. Lett.*, 2012, **1**, H17-H19.
4 D. Li, T. Liu, Z. Yan, L. Zhen, J. Liu, J. Wu and Y. Feng, *ACS Appl. Mater. Interfaces*, 2020, **12**, 7030-7037.
5 R. A. Geioushy, M. M. Khaled, K. Alhooshani, A. S. Hakeem and A. Rinaldi, *Electrochim. Acta*, 2017, **245**, 456-462.
6 B. Zhang, Z. Guo, Z. Zuo, W. Pan and J. Zhang, *Applied Catalysis B: Environmental*, 2018, **239**, 441-449.
7 Z. Chen, K. Mou, X. Wang and L. Liu, *Angew Chem Int Ed Engl*, 2018, **57**, 12790-12794.
8 J. Huang, X. Guo, G. Yue, Q. Hu and L. Wang, *ACS Appl. Mater. Interfaces*, 2018, **10**, 44403-44414.
9 Z. Chen, K. Mou, S. Yao and L. Liu, *ChemSusChem*, 2018, **11**, 2944-2952.
10 H. Ning, Q. Mao, W. Wang, Z. Yang, X. Wang, Q. Zhao, Y. Song and M. Wu, *Journal of Alloys and Compounds*, 2019, **785**, 7-12.